PCR led us to the suggestion that SYP expression in adrenocortical adenomas may be associated with functions such as the transport or secretion of at least glucocorticoids. However, not all cases conformed to our postulation, because there was one case each among the APA and NFA cases in which there was an intense SYP immunoreactivity (staining scores 3 and 2), but no oversecretion of cortisol. Adrenocortical tumors have also been known to express some neuropeptides (34, 35), and, hence, the possibility that SYP expression may be related to the secretion of neuropeptides cannot be completely ruled out. Further investigation into SYP expression in adrenocortical lesions, especially *in vivo* experiments, is required.

Declaration of interest

The authors declare that there is no conflict of interest that could be perceived as prejudicing the impartiality of the research reported.

Funding

This research did not receive any specific grant from any funding agency in the public, commercial, or not-for-profit sector.

Acknowledgements

The authors thank Mrs Amanda Nishida for critical comments and Mrs Kanako Hayashi for technical assistance.

References

1 d'Alva CB, Abiven-Lepage G, Viallon V, Groussin L, Dugue MA, Bertagna X & Bertherat J. Sex steroids in androgen-secreting adrenocortical tumors: clinical and hormonal features in comparison with non-tumoral causes of androgen excess. *European Journal of Endocrinology* 2008 **159** 641–647.
2 Saadi HF, Bravo EL & Aron DC. Feminizing adrenocortical tumor: steroid hormone response to ketoconazole. *Journal of Clinical Endocrinology and Metabolism* 1990 **70** 540–543.
3 Aiba M, Hirayama A, Iri H, Ito Y, Fujimoto Y, Mabuchi G, Murai M, Tazaki H, Maruyama H, Saruta T, Suda T & Demura H. Adrenocorticotropic hormone-independent bilateral adrenocortical macronodular hyperplasia as a distinct subtype of Cushing's syndrome. Enzyme histochemical and ultrastructural study of four cases with a review of the literature. *American Journal of Clinical Pathology* 1991 **96** 334–340.
4 Aiba M, Okamoto T, Ito Y, Obara T, Kameyama K, Mitani F & Ishimura Y. Cytochrome P450aldo, P45011β, and 3-β-hydroxysteroid dehydrogenase (3βHSD) in adrenal cortices and tumor. *Pathology International* 2000 **50** (Suppl) A63 (Abstract).
5 Sasano H. Localization of steroidogenic enzymes in adrenal cortex and its disorders. *Endocrine Journal* 1994 **41** 471–482.
6 Shigematsu K, Kawai K, Irie J, Sakai H, Nakashima O, Iguchi A, Shimamatsu J, Shimamatsu K, Kusaba Y & Takahara O. Analysis of unilateral adrenal hyperplasia with primary aldosteronism from the aspect of messenger ribonucleic acid expression for steroidogenic enzymes: a comparative study with adrenal cortices adhering to aldosterone-producing adenoma. *Endocrinology* 2006 **147** 999–1006.
7 Shigematsu K, Nakagaki T, Yamaguchi N, Kawai K, Sakai H & Takahara O. Analysis of mRNA expression for steroidogenic enzymes in the remaining adrenal cortices attached to adrenocortical adenomas. *European Journal of Endocrinology* 2008 **158** 867–878.
8 Nylen ES & Becker KL. The diffuse neuroendocrine system. In *Principles and Practice of Endocrinology and Metabolism*, pp 1276–1283. Ed. KL Becker, J. B. Lippincott Company: Philadelphia, 1990.
9 Miettinen M. Neuroendocrine differentiation in adrenocortical carcinoma. New immunohistochemical findings supported by electron microscopy. *Laboratory Investigation* 1992 **66** 169–174.
10 Haak HR & Fleuren G-J. Neuroendocrine differentiation of adrenocortical tumors. *Cancer* 1995 **75** 860–864.
11 Komminoth P, Roth J, Schröder S, Saremaslani P & Heitz PU. Overlapping expression of immunohistochemical markers and synaptophysin mRNA in pheochromocytomas and adrenocortical carcinomas. Implications for the differential diagnosis of adrenal gland tumors. *Laboratory Investigation* 1995 **72** 424–431.
12 Ehrhart-Bornstein M & Hilbers U. Neuroendocrine properties of adrenocortical cells. *Hormone and Metabolic Research* 1998 **30** 436–439.
13 Li Q, Johansson H, Kjellman M & Grimelius L. Neuroendocrine differentiation and nerves in human adrenal cortex and cortical lesions. *Acta Pathologica, Microbiologica, et Immunologica Scandinavica* 1998 **106** 807–817.
14 Wiedenmann B & Franke WW. Identification and localization of synaptophysin, an integral membrane glycoprotein of Mr 38,000 characteristic of presynaptic vesicles. *Cell* 1985 **41** 1017–1028.
15 Wiedenmann B, Franke WW, Kuhn C, Moll R & Gould VE. Synaptophysin: a marker protein for neuroendocrine cells and neoplasms. *PNAS* 1986 **83** 3500–3504.
16 Leube RE. Expression of the synaptophysin gene family is not restricted to neuronal and neuroendocrine differentiation in rat and human. *Differentiation* 1994 **56** 163–171.
17 Maggiano N, Lauriola L, Serra FG, Ricci R, Capelli A & Ranelletti FO. Detection of synaptophysin-producing cells in human thymus by immunohistochemistry and nonradioactive *in situ* hybridization. *Journal of Histochemistry and Cytochemistry* 1994 **47** 237–243.
18 Ronn LC, Hartz BP & Bock E. The neural cell adhesion molecule (NCAM) in development and plasticity of the nervous system. *Experimental Gerontology* 1998 **33** 853–864.
19 Walsh FS & Doherty P. Neural cell adhesion molecules of the immunoglobulin superfamily: role in axon growth and guidance. *Annual Review of Cell and Developmental Biology* 1997 **13** 425–456.
20 Lahr G, Mayerhoffer A, Bucher S, Barthels D, Wille W & Gratzl M. Neural cell adhesion molecules in rat endocrine tissues and tumor cells: distribution and molecular analysis. *Endocrinology* 1993 **132** 1207–1217.
21 Muench MO, Ratcliffe JV, Nakanishi M, Ishimoto H & Jaffe RB. Isolation of definitive zone and chromaffin cells based upon expression of CD56 (neural cell adhesion molecule) in the human fetal adrenal gland. *Journal of Clinical Endocrinology and Metabolism* 2003 **88** 3921–3930.
22 Weiss LM. Comparative histologic study of 43 metastasizing and nonmetastasizing adrenocortical tumors. *American Journal of Surgical Pathology* 1984 **8** 163–169.
23 Weiss LM, Medeiros LJ & Vickery AL Jr. Pathologic features of prognostic significance in adrenocortical carcinoma. *American Journal of Surgical Pathology* 1989 **13** 202–206.
24 Shigematsu K, Katamine S, Nakatani A, Niwa M, Kataoka Y, Kamio T & Kawai K. Immunohistochemical evidence for protein kinase C in primary human adrenal tumors. *Acta Histochemica et Cytochemica* 1992 **25** 511–522.
25 Mesiano S, Coulter CL & Jaffe RB. Localization of cytochrome P450 cholesterol side-chain cleavage, cytochrome P450 17α-hydroxylase/17, 20-lyase, and 3β-hydroxysteroid dehydrogenase isomerase steroidogenic enzymes in human and rhesus monkey fetal adrenal glands: reappraisal of functional zonation. *Journal of Clinical Endocrinology and Metabolism* 1993 **77** 1184–1189.

26 Buffa R, Rindi G, Sessa F, Gini A, Capella C, Jahn R, Navone F, De Camilli P & Solcia E. Synaptophysin immunoreactivity and small clear vesicles in neuroendocrine cells and related tumours. *Molecular and Cellular Probes* 1987 **1** 367–381.

27 Pelletier G, Li S, Luu-The V, Tremblay Y, Bélanger A & Labrie F. Immunoelectron microscopic localization of three key steroidogenic enzymes (cytochrome P450(scc) 3β-hydroxysteroid dehydrogenase and cytochrome P450(c17)) in rat adrenal cortex and gonads. *Journal of Endocrinology* 2001 **171** 373–383.

28 Nussdorfer GG. Cytophysiology of adrenal cortex. *International Review of Cytology* 1986 **98** 1–405.

29 Cheng B & Kowal J. Role of the Golgi complex in adrenocortical steroidogenesis. *Microscopy Research and Technique* 1997 **36** 503–509.

30 Bassett JR & Pollard I. The involvement of coated vesicles in the secretion of corticosterone by the zona fasciculata of the rat adrenal cortex. *Tissue & Cell* 1980 **12** 101–115.

31 Alsabeh R, Mazoujian G, Goates J, Medeiros LJ & Weiss LM. Adrenal cortical tumors clinically mimicking pheochromocytoma. *American Journal of Clinical Pathology* 1995 **104** 382–390.

32 Stratakis CA, Carney JA, Kirschner LS, Willenberg HS, Brauer S, Ehrhart-Bornstein M & Bornstein SR. Synaptophysin immunoreactivity in primary pigmented nodular adrenocortical disease: neuroendocrine properties of tumors associated with Carney complex. *Journal of Clinical Endocrinology and Metabolism* 1994 **84** 1122–1128.

33 Shigematsu K. Comparative studies between hormone contents and morphological appearances in human adrenal cortex – special reference to non-functioning tumors (adenoma and adenomatous nodule) and functioning adenoma. *Acta Histochemica et Cytochemica* 1982 **15** 386–400.

34 Fukuda T, Takahashi K, Suzuki T, Saruta M, Watanabe M, Nakata T & Sasano H. Urocortin 1, urocortin 3/stresscopin, and corticotrophin-releasing factor receptors in human adrenal and its disorders. *Journal of Clinical Endocrinology and Metabolism* 2005 **90** 4671–4678.

35 Morimoto R, Satoh F, Murakami O, Hirose T, Totsune K, Imai Y, Arai Y, Suzuki T, Sasano H, Ito S & Takahashi K. Expression of adrenomedullin 2/intermedin in human adrenal tumors and attached non-neoplastic adrenal tissues. *Journal of Endocrinology* 2008 **198** 175–183.

Received 21 August 2009
Accepted 14 September 2009

Endocr Pathol (2009) 20:66–72
DOI 10.1007/s12022-009-9060-8

Primary Aldosteronism with Aldosterone-Producing Adenoma Consisting of Pure Zona Glomerulosa-Type Cells in a Pregnant Woman

Kazuto Shigematsu · Noriyuki Nishida · Hideki Sakai · Tsukasa Igawa · Shin Suzuki · Kioko Kawai · Osamu Takahara

Published online: 6 February 2009

Abstract Aldosterone-producing adenoma (APA) consisting of pure zona glomerulosa (ZG)-type cells is extremely rare, and primary aldosteronism complicated by pregnancy is also rare. We report a case of APA discovered in a 32-year-old pregnant woman who visited our hospital for hypertension and hypokalemia at 26 weeks gestation. Elevated plasma aldosterone concentration and hypokalemia were observed, and an magnetic resonance imaging scan demonstrated a right adrenal mass. A laparoscopic adrenalectomy was performed because of refractory hypokalemia. Pathologically, the adrenal mass was diagnosed as APA, and in addition to the cytological features, in situ hybridization and real-time polymerase chain reaction proved that all the component cells were ZG-type cells. The cells also showed estrogen receptor β immunoreactivity and melanocortin 2 receptor mRNA expression, suggesting that estrogen and/or ACTH might be related to the proliferation of APA cells during pregnancy. Our case is the first report of APA consisting of ZG-type cells discovered during pregnancy.

Keywords primary aldosteronism · aldosterone-producing adenoma · zona glomerulosa-type cells · pregnancy · sex steroid hormone receptor · ACTH

K. Shigematsu · O. Takahara
Department of Pathology, Japanese Red-Cross Nagasaki Atomic Bomb Hospital,
Nagasaki 852-8511, Japan

N. Nishida
Division of Molecular Microbiology and Immunology, Nagasaki University Graduate School of Biomedical Sciences,
Nagasaki 852-8523, Japan

H. Sakai · T. Igawa
Division of Nephro-Urology, Nagasaki University Graduate School of Biomedical Sciences,
Nagasaki 852-8523, Japan

S. Suzuki
Department of Cardiovascular Internal Medicine, Nagasaki Municipal Hospital,
Nagasaki 850-8555, Japan

K. Kawai
Department of Pathology, Nagasaki Prefecture Medical Health Operation Group,
Isahaya 859-0401, Japan

K. Shigematsu (✉)
Division of Pathology, Nagasaki University Graduate School of Biomedical Sciences,
1-12-4 Sakamoto,
Nagasaki 852-8523, Japan
e-mail: shigek@net.nagasaki-u.ac.jp

Introduction

Primary aldosteronism (PA) is an important surgically curable cause of hypertension resulting from excess aldosterone production and is rarely associated with pregnancy [1]. Hypertension and electrolyte abnormality are risk factors to both mother and fetus [2], so an effective treatment is imperative. However, the data in a pregnant patient with PA may be difficult to interpret because all components of the renin–angiotensin–aldosterone system (RAAS) are stimulated during normal pregnancy [3].

Most PA is caused by either aldosterone-producing adenoma (APA) or bilateral adrenal hyperplasia (BAH) [4]. Microscopically, APA consists predominantly of large lipid-laden clear-type cells resembling those of the zona fasciculata (ZF) and smaller clear-type cells featuring the

Humana Press

cytological characteristics of both zona glomerulosa (ZG) and ZF cells (so-called hybrid or intermediate-type cells) [5]. Recognizable ZG-type cells are also present in many APAs, but it is extremely rare that ZG-type cells are the sole component of APA [5]. This report deals with a case of APA consisting uniquely of ZG cells discovered during pregnancy.

Case Report

A 32-year-old woman visited her local hospital at 11 weeks gestation for hypertension (168/99 mmHg). Her past history did not include hypertension, but how long the hypertension had existed could not be confirmed. Hypokalemia (2.0 mEq/l) was detected at 18 weeks gestation. Proteinuria and peripheral edema were subsequently noted at 24 weeks gestation. On the workup, she was discovered to have an elevated plasma aldosterone concentration (PAC; 82.6 ng/ml; normal value, 3.6–24.0 ng/dl), and an magnetic resonance (MRI) scan disclosed a right adrenal mass measuring about 1.5 cm in diameter. She was referred to our hospital for management of hypertension and hypokalemia. At admission, her blood pressure (BP) was 140–150/90–100 mmHg. There was no specific finding in the physical examination, but the serum potassium was low (2.3 mEq/l). Hormonal evaluation revealed elevated PAC (1,270 pg/ml; normal value, 29.9–159 pg/ml), while the plasma renin was within the normal range (4.2 pg/ml; normal value, 2.5–21 pg/ml). The plasma cortisol (F) was normal (17.5 μg/dl; normal value, 4.5–21.1 μg/dl), and there was no loss of circadian rhythm. She was diagnosed as having PA caused by the right adrenal mass, although further examinations were not done because of her pregnancy. A laparoscopic right adrenalectomy was performed at 26 weeks gestation, as the hypokalemia was resistant to aggressive potassium supplementation. After surgery, PAC and potassium levels rapidly improved, but the BP remained elevated at 140–150/90–100 mmHg. At no point was any abnormality detected in the fetus, and the baby was safely born by cesarean at 38 weeks gestation.

Materials and Methods

The patient signed a form of informed consent prepared in accordance with the rules outlined by the Nagasaki University Ethics Committee. Tissues were fixed in 10% buffered formalin and stained with hematoxylin and eosin. Immunohistochemical stains were performed using paraffin-embedded sections and antibodies directed against MIB-1 (Dako, Tokyo, Japan), estrogen receptor α (ERα) (Dako), estrogen receptor β (ERβ) (Dako), progesterone receptor (PgR; Dako), and angiotensin II type-1 receptor (AT1; Assay Designs, Inc., MI). Normal mouse or rabbit IgG was used instead of the primary antibody as a negative control. The number of MIB-1 positive nuclei per 1,000 total tumor nuclei was counted and the percentage of positive nuclei determined.

In situ hybridization was performed as described previously [6]. cDNA fragments of melanocortin 2 receptor (MC2R), steroidogenic acute regulatory protein (StAR), CYP11A1, HSD3B2, CYP11B, CYP17A1, and CYP21A2 were obtained by reverse transcriptase-polymerase chain reaction and subcloned into pT-NOT vector [6]. Antisense and sense strand cRNAs were synthesized using Digoxigenin (DIG)-UTP (Roche Diagnostics, Germany) with T3 or T7 RNA polymerase (Takara, Otsu, Japan). Four-micrometer-thick paraffin sections were hybridized with DIG-labeled cRNA probes at 42°C for 16 h and finally washed in 0.2× SCC at 50°C for 20 min. Hybridization signals were immunologically detected with alkaline phosphatase-conjugated anti-DIG Fab fragments (diluted 1:500; Roche Diagnostics).

To determine the expression of CYP11B1, CYP11B2, and CYP17A1 encoding 11β-hydroxylase, aldosterone synthase, and 17α-hydroxylase, respectively, we performed real-time polymerase chain reaction (PCR) amplification. Sequence-specific primers were designed as previously described [6]. Expression levels were standardized to 18S rRNA. Total RNA was collected from frozen tumor and its remaining adrenal gland tissues using GenElute Mammalian Total RNA kit (Sigma-Aldrich Inc., Tokyo). After the reverse transcriptase reaction, LightCycler Quick System 330 (Roche Diagnostic Co., Tokyo, Japan) was used for the real-time PCR. Relative quantitation of gene expression was performed using the relative standard curve method. As controls, APAs (PAC, 249–650 pg/ml; normal value, 29.9–159 pg/ml; F, 6–10 μg/ml; normal value, 4.5–21.1 μg/dl), and cortisol-producing adenomas (CPAs; PAC, 3–20 pg/ml; F, 22–25 μg/ml) were also examined.

Results

Macroscopic and Microscopic Features

The resected right adrenal contained a golden yellow colored tumor, which was 1.1 cm in size (Fig. 1a). The tumor was well circumscribed without capsulation and was found to be composed of small clear-type and compact-type cells forming alveoli, solid trabeculae, and pseudotubules (Fig. 1b, c). Stromal myxomatous change was also present together with prominent vascular sinusoids. There was compressed adrenal cortex on part of the surface. Pathologically, the tumor was diagnosed as an adrenocortical adenoma according to the histopathologic criteria proposed by Weiss et al. [7]. The remaining adrenal cortex did not

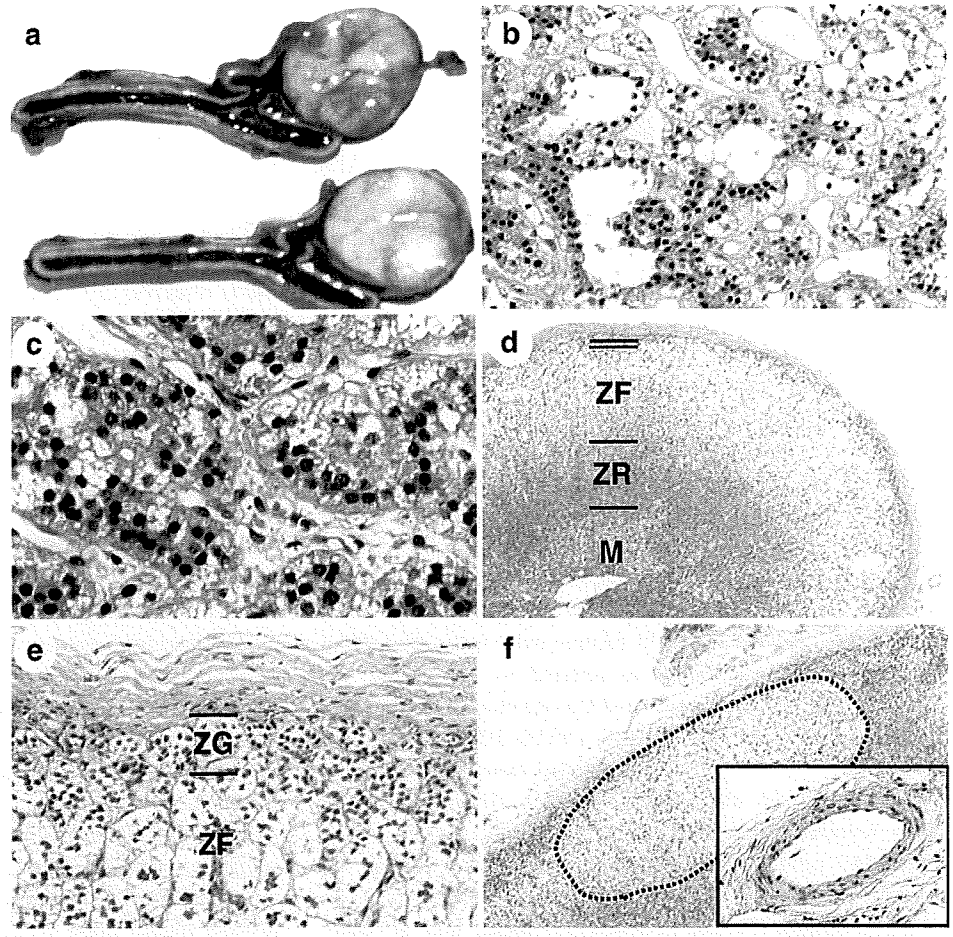

Fig. 1 On macroscopic examination (**a**), the resected right adrenal contained a golden yellow colored tumor measuring about 1.1 cm in diameter. The adenoma was well circumscribed without capsulation and was found to be composed of cells resembling the ZG cells, which formed alveoli, solid trabeculae, and pseudotubules (**b**, **c**). The remaining adrenal cortex did not show hyperplasia of ZG (**d**, **e**). Small cortical nodules consisting of ZF cells were observed (**f**), but there was no obvious thickening of the vascular wall (**f**, *insert*). *ZG* zona glomerulosa, *ZF* zona fasciculate, *ZR* zona reticularis, *M* medulla; **b** ×200; **c** ×400; **d** ×4; **e** ×200; **f** ×40; *square box* in **f** ×200

show hyperplasia or atrophy of ZG (Fig. 1d, e), but several small cortical nodules consisting of ZF cells were observed (Fig. 1f). There was no obvious thickening of the vascular wall (Fig. 1f, square box).

Immunohistochemistry and in Situ Hybridization

The adenoma cells were positive for MIB-1 (Fig. 2a), defined as 4.9 % positive nuclei. Among the steroid receptors, the expression for ERβ was observed in all adenoma cells (Fig. 2b) and the ZG and ZF cells of the adrenal cortex. On the other hand, ERα was detected in neither adenoma cells nor the cortex (data not shown). PgR was focally expressed in the outer ZF cells, but not adenoma cells (data not shown). A few adenoma cells showed immunoreactivity for AT1 (Fig. 2c). The faint expression of MC2R mRNA was also found in many adenoma cells (Fig. 2d). In situ hybridization indicated that the adenoma cells intensely expressed mRNAs for StAR (data not shown), CYP11A1 (data not shown), HSD3B2 (Fig. 2e, i), CYP11B (Fig. 2f, j), and CYP21A2 (Fig. 2h, l), but not CYP17A1 (Fig. 2g, k). On the other hand, the adrenal cortex attached to the adenoma demonstrated the expression of all mRNAs in the inner ZF to ZR, but not in the ZG to outer ZF (Fig. 2m–p).

Real-Time PCR

The real-time PCR demonstrated that the level of CYP11B1 mRNA was very low in the adenoma tissue (Fig. 3a), whereas that of CYP11B2 mRNA in the adenoma tissue was higher than typically found in APAs and CPAs (Fig. 3b). Therefore, the majority of CYP11B signals detected by in situ hybridization were thought to be CYP11B2 mRNA. The level of CYP17A1 mRNA expression in the adenoma tissue was extremely low (Fig. 3c), supporting the findings of the in situ hybridization. On the other hand, the remaining adrenal cortex showed high levels of CYP11B1 and CYP17A1, and a low level of CYP11B2, compared with levels in the adenoma tissue (Fig. 3).

Discussion

The discovery of PA during pregnancy is rare, and fewer than 30 cases have been described in the English-language

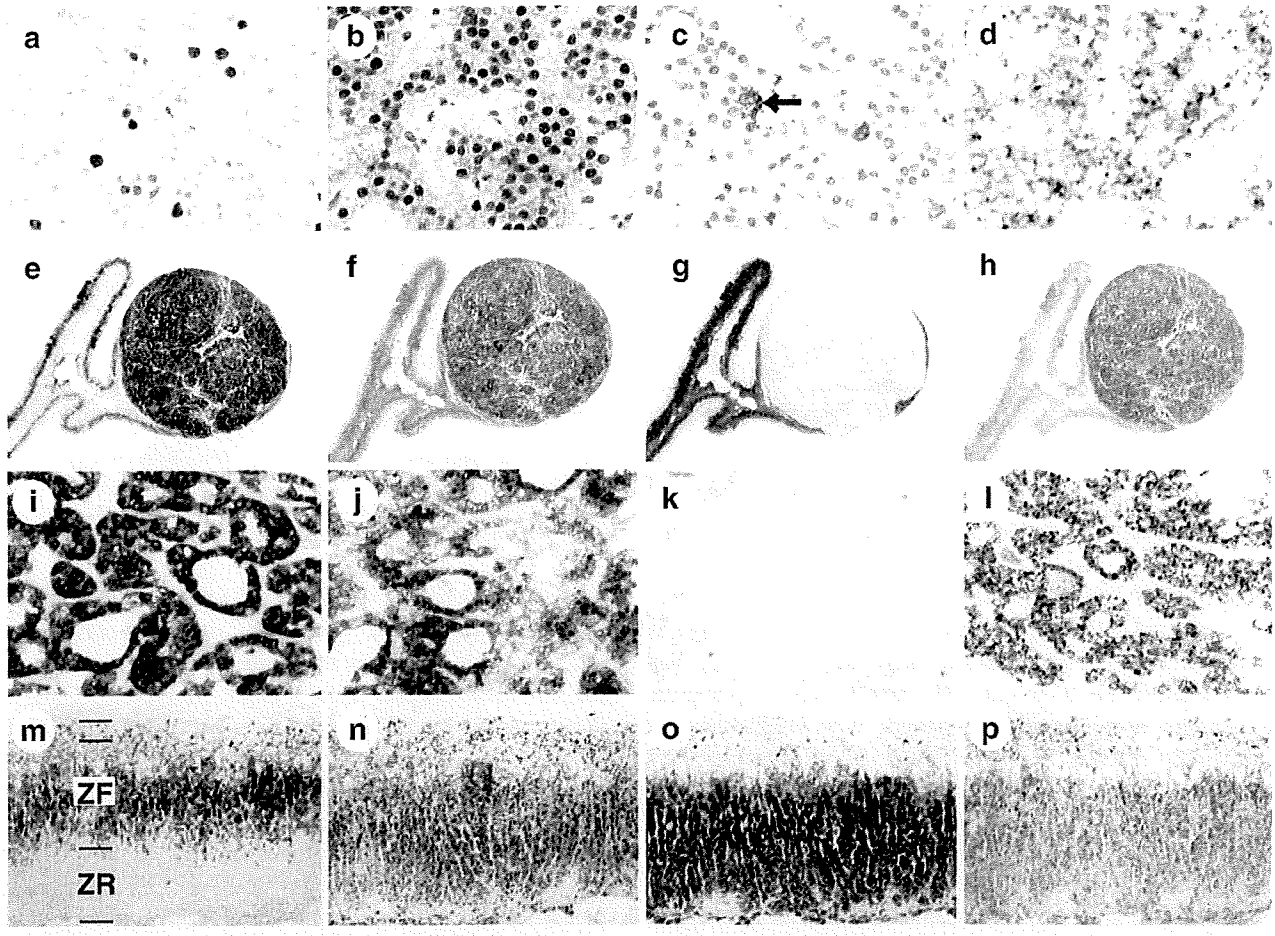

Fig. 2 The MIB-1 index was 4.9 % in the adenoma (**a**). Among sex steroid receptors, ERβ (**b**) was observed in all adenoma cells. A few cells expressed AT1 (**c**, *arrow*), whereas the expression of MC2R mRNA (**d**) was faint but found in many cells. The adenoma expressed mRNAs for StAR, CYP11A1, HSD3B2 (**e**, **i**), CYP11B (**f**, **j**), and CYP21A2 (**h**, **l**), but not CYP17A1 (**g**, **k**). The remaining adrenal cortex demonstrated the expression of HSD3B2 (**m**), CYP11B (**n**), CYP17A1 (**o**), and CYP21A2 (**p**) in the ZF to ZR, but not in the ZG. *ZG* zona glomerulosa, *ZF* zona fasciculate, *ZR* zona reticularis. **a–d**, ×400; **e–h** ×1; **i–l** ×200; **m–p**, ×100

literature [1]. Several factors complicate the diagnosis of PA during pregnancy. Hypertension is a fairly common complication of pregnancy, and normal pregnancy is characterized by enhanced RAAS [1], resulting in elevated PAC. Additionally, more thorough examinations such as I^{131}-aldosterol scintigram, adrenal venous sampling and loading tests are contraindicated during pregnancy. In our case, a sufficient workup could not be done, but the diagnosis of PA was given in view of the presence of a right adrenal mass demonstrated by an MRI scan in association with elevated PAC and hypokalemia.

In this case, the plasma renin level was within the normal range, whereas most patients with PA show low plasma renin levels as well as elevated PAC. Okawa et al. [8] reported that the normoreninemia in pregnant patients with PA was associated with placental abruption or preterm birth along with fetal growth restriction and poor outcome. In our patient, hypertension remained even after adrenalectomy, although the fetus appeared to remain free of any abnormalities. The reason for these discrepancies is unclear. Laidlaw et al. [9] reported that the progressively increasing progesterone during pregnancy blocked the effects of aldosterone at the renal tubule and successfully reduced BP in patients with PA. Increased prostaglandin activity is also believed to mediate the pressor effects of angiotensin II in the maternal vasculature [3, 10]. On the other hand, estrogen stimulates hepatic angiotensinogen, which is the precursor of angiotensin I, and thus renin secretion [10]. Therefore, it is considered that during pregnancy, the balance between aldosterone and other steroids may determine whether hypertension and hypokalemia are improved or become exacerbated and whether the PRA remains suppressed.

Pathologically, the remaining adrenal cortex did not show atrophy or hyperplasia except for several small cortical nodules. In situ hybridization and real-time PCR

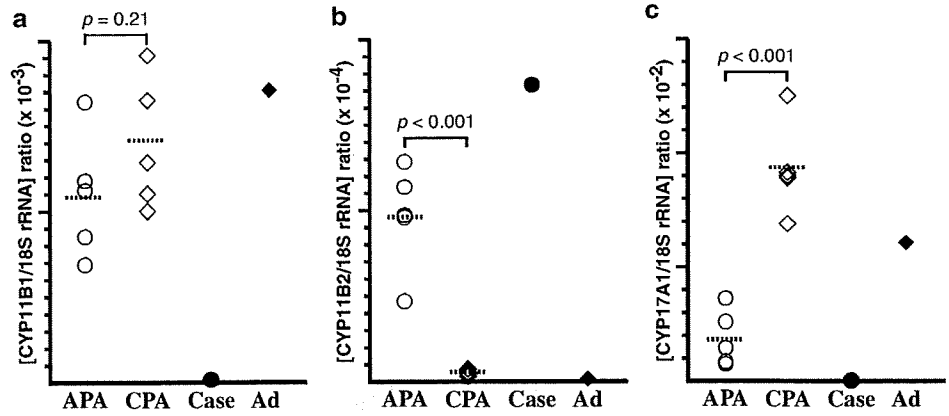

Fig. 3 Analysis of CYP11B1 (**a**), CYP11B2 (**b**), and CYP17A1 (**c**) expression by real-time PCR. The results are shown as the ratio of CYP11B1, CYP11B2, or CYP17A1 to 18S rRNA. The *dotted lines* show the mean value in APA and CPA tissues, respectively. Differences were analyzed with Student's *t* test. APA (*empty circle*), aldosterone-producing adenoma; CPA (*empty diamond*), cortisol-producing adenoma; case (*filled circle*), APA in our patient; Ad (*filled diamond*), remaining adrenal gland in our patient

showed that glucocorticoid synthesis was well sustained, whereas the mRNA expression for steroidogenic enzymes including CYP11B2, encoding aldosterone synthase, was restrained in the ZG to outer ZF, thereby indicating that the adenoma observed in our patient was functional and consistent with APA [6]. In many APAs, ZG-type cells are predominantly observed around the periphery of the lesion, dipping into the inside of the adenoma in a tongue-like manner [5]. On the other hand, the APA in our patient consisted only of smaller cells, which were cytologically consistent with ZG-type cells. In situ hybridization demonstrated that these intensely expressed mRNAs for StAR, CYP11A1, HSD3B2, CYP11B, and CYP21A2, but not CYP17A1, and the real-time PCR proved that CYP11B2 mRNA was the main component of CYP11B detected by in situ hybridization. Therefore, in addition to the cytological features, the expression pattern of steroidogenic enzymes also showed that the APA in our patient consisted of only ZG-type cells [11]. APA consisting of pure ZG-type cells is extremely rare, since most APAs consist predominantly of ZF-like and hybrid cells [5].

When the APA formation in our patient had occurred was unclear. The presence of PA came to light for the first time during the pregnancy, but as at least 30 doubling times are needed to develop to 10^9 cells (tumor of about 1-cm size) from a single cell [11], it would seen more likely that the adenoma or precursor lesion was already present before pregnancy rather than developing only during the pregnancy. Subcapsular micronodules with similar cytological features are often observed in non-tumorous adrenal cortices and have been thought to be incidental and nonfunctional, probably related to vascular sclerosis [12]. However, we have recently proved by in situ hybridization and real-time PCR that at least some microscopic subcapsular micronodules have the ability to actively produce aldosterone, as observed in BAH and unilateral adrenal hyperplasia (UAH) [6]. With this in mind, the present case would support our theory that a micronodule burgeoning in the subcapsular region initially might ultimately become an adenoma, causing PA.

The MIB-1 index in our case was 4.9 %, which was less than that in adrenocortical carcinomas, but a relatively high score compared with a typical adrenocortical adenoma [13]. In addition to RAAS components and sex hormones [3], it is well known that substances such as ACTH-like compound are secreted by the placenta [14]. We examined by immunohistochemistry and in situ hybridization whether sex hormones, angiotensin II, and ACTH were related to the proliferation of APA cells. Immunoreactivity for ERβ, but not ERα or PgR, was detected in all cells of APA. The expression of MC2R mRNA, encoding the receptor for ACTH, was observed only faintly but in many cells of the APA. On the other hand, AT1 was present in only a few cells. Therefore, progesterone and angiotensin II (through AT1) seemed not to be directly involved in the proliferation of APA cells. On the other hand, the expression of ERβ and MC2R has also been reported in several cases of adrenocortical tumors unassociated with pregnancy [15, 16]. ACTH and MC2R are required for adrenal gland development and steroidogenesis [17, 18]. Georgiadou et al. [19] showed that in men as well as in women, ERβ was detected in many APAs (seven of nine cases), whereas ERα was negative in all the APAs examined. Therefore, the expression of ERβ and MC2R might be not specific to our case. However, the highly estrogenic environment during pregnancy has been reported to influence the development and streoidogenesis of the fetal adrenal gland, probably through ERβ [20]. Montanaro et al. [21] demonstrated that the H295R adrenocortical carcinoma cell line expressed cytochrome P450 aromatase and estrogen receptors (with more

mRNA expression for ERβ than for ERα) and that 17β-estradiol enhanced adrenocortical cell proliferation. Taken together with the evidence that the levels of estrogen and ACTH are higher in pregnant than in non-pregnant patients [3], it is possible that estrogen and ACTH, through ERβ and MC2R, respectively, might participate in the proliferation, and eventually active steroidogenesis, in APA cells to a greater degree in pregnancy than in non-pregnancy.

The overexpression of CYP11B2 and CYP17A1 mRNAs in APAs and CPAs, respectively, is well known [22]. The expression level of CYP11B2 mRNA in the APA of our patient was higher than that in APAs examined as controls, reflecting well the difference in PAC values (1,270 pg/ml versus 249–650 pg/ml). In contrast, the expression level of CYP11B1 mRNA, encoding 11β-hydroxylase, the limiting enzyme in cortisol biosynthesis [18, 22], in the control APAs was higher than that in our case. Most APAs have the potential for cortisol as well as aldosterone synthesis [23], while the APA in our patient consisted of only ZG-type cells with no potential for cortisol synthesis [11]. Therefore, it is no surprise that typical APAs expressed CYP11B1 mRNA at higher levels than in our case.

To our knowledge, the particular constellation of clinical and biological features presenting in our patient has not been reported elsewhere. A similar pattern of expression of steroidogenic enzymes is observed in BAH and UAH, including unilateral multiple adrenocortical micronodules in which the endocrinologic findings, if not the roentgenologic findings, are quite similar to those of typical APAs [6, 24]. Therefore, it may be difficult to differentiate the APA seen in our patient from the typical APAs by clinical and biological features.

The presence of PA is perilous for both mother and fetus, and it is thus necessary to keep in mind that careful investigation must be performed when hypertension and electrolyte abnormality are noted during pregnancy. Our case is the first report of APA consisting of purely ZG-type cells discovered during pregnancy and is invaluable in the study of APA formation. Further examinations are required to elucidate the mechanism of development of APA in pregnant patients.

Acknowledgments The authors thank Mrs. Amanda Nishida for critical comments and Mrs. Kanako Hayashi for technical assistance. The authors did not receive any funding concerning this manuscript and declare that there is no conflict of interest that would prejudice its impartiality.

References

1. Kosaka K, Onoda N, Ishikawa T, Iwanaga N, Yamamasu S, Tahara H, Inaba M, Ishimura E, Ogawa Y, Hirakawa K. Laparoscopic adrenalectomy on a patient with primary aldosteronism during pregnancy. Endcr J 53:461–6, 2006 doi:10.1507/endocrj.K05-122.
2. August P, Lindheimer MD. Hypertension in pregnancy. In: Kaplan NM, et al, ed. Individualized therapy of hypertension. New York: Marcel Dekker, pp. 165–93, 1995.
3. Wilson M, Morganti AA, Zervoudakis I, Letcher RL, Romney BM, Von Oeyon P, Papera S, Sealey JE, Laragh JH. Blood pressure, the renin–aldosterone system and sex steroids throughout normal pregnancy. Am J Med 68:97–104, 1980 doi:10.1016/0002-9343(80)90178-3.
4. Magill SB, Raff H, Shaker JL, Brickner RC, Knechtges TE, Kehoe ME, Findling JW. Comparison of adrenal vein sampling and computed tomography in the differentiation of primary aldosteronism. J Clin Endocrinol Metab 86:1066–71, 2001 doi:10.1210/jc.86.3.1066.
5. Neville AM, O'Hare MJ. Hyperaldosteronism and related syndromes of mineralocorticoid excess. In: Neville AM, et al, ed. The human adrenal cortex. Berlin: Springer, pp. 202–41, 1982.
6. Shigematsu K, Nakagaki T, Yamaguchi N, Kawai K, Sakai H, Takahara O. Analysis of mRNA expression for steroidogenic enzymes in the remaining adrenal cortices attached to adrenocortical adenomas. Eur J Endocrinol 158:867–78, 2008 doi:10.1530/EJE-07-0626.
7. Weiss LM, Medeiros LJ, Vickery AL Jr. Pathologic features of prognostic significance in adrenocortical carcinoma. Am J Surg Pathol 13:202–6, 1989.
8. Okawa T, Asano K, Hashimoto T, Fujimori K, Yanagida K, Sato A. Diagnosis and management of primary aldosteronism in pregnancy: case report and review of the literature. Am J Perinatol 19:31–6, 2002 doi:10.1055/s-2002-20170.
9. Laidlaw JC, Ruse JL, Gornall AG. The influence of estrogen and progesterone on aldosterone excretion. J Clin Endocrinol Metab 22:161–71, 1962.
10. Casey ML, MacDonald PC, Simpson ER. Endocrinological changes of pregnancy. In: Wilson JD, et al, ed. Williams textbook of endocrinology. 8th ed. Philadelphia: Saunders, pp. 977–91, 1996.
11. Aiba M, Fujibayashi M. Histopathological diagnosis and prognostic factors in adrenocortical carcinoma. Endocr Pathol 16:13–22, 2005 doi:10.1385/EP:16:1:013.
12. Dobbie JW. Adrenocortical nodular hyperplasia: the ageing adrenal. J Pathol 99:1–18, 1969 doi:10.1002/path.1710990102.
13. Schmitt A, Saremaslani P, Schmid S, Rousson V, Montani M, Schmid DM, Heitz PU, Komminoth P, Perren A. IGFII and MIB1 immunohistochemistry is helpful for the differentiation of benign from malignant adrenocortical tumours. Histopathology 49:298–307, 2006 doi:10.1111/j.1365-2559.2006.02505.x.
14. Keegan GT, Grabarits F, Roland AS. Pregnancy complicated by Cushing's syndrome. South Med J 69:1207–9, 1976.
15. Allolio B, Reincke M. Adrenocorticotropin receptor and adrenal disorders. Horm Res 47:273–8, 1997 doi:10.1159/000185476.
16. de Cremoux P, Rosenberg D, Goussard J, Brémont-Weil C, Tissier F, Tran-Perennou C, Groussin L, Bertagna X, Bertherat J, Raffin-Sanson ML. Expression of progesterone and estradiol receptors in normal adrenal cortex, adrenocortical tumors, and primary pigmented nodular adrenocortical disease. Endocr Relat Cancer 15:465–74, 2008 doi:10.1677/ERC-07-0081.
17. Chida D, Nakagawa S, Nagai S, Sagara H, Katsumata H, Imaki T, Suzuki H, Mitani F, Ogishima T, Shimizu C, Kotaki H, Kakuta S, Sudo K, Koike T, Kubo M, Iwakura Y. Melanocortin 2 receptor is required for adrenal gland development, steroidogenesis, and neonatal gluconeogenesis. Proc Natl Acad Sci U S A 104:18205–10, 2007 doi:10.1073/pnas.0706953104.
18. Sewer MB, Waterman MR. ACTH modulation of transcription factors responsible for steroid hydroxylase gene expression in the

adrenal cortex. Microsc Res Tech 61:300–7, 2003 doi:10.1002/jemt.10339.
19. Georgiadou D, Sergentanis TN, Kostopoulou A, Zografos GN, Papastratis G. Estrogen receptors alpha and beta in adrenal cortical neoplasia: heterogeneity and physiological implications. Virchows Arch 452:181–91, 2008 doi:10.1007/s00428-007-0542-0.
20. Albrecht ED, Babischkin JS, Davies WA, Leavitt MG, Pepe GJ. Identification and developmental expression of the estrogen receptor alpha and beta in the baboon fetal adrenal gland. Endocrinology 140:5953–61, 1999 doi:10.1210/en.140.12.5953.
21. Montanaro D, Maggiolini M, Recchia AG, Sirianni R, Aquila S, Barzon L, Fallo F, Andò S, Pezzi V. Antiestrogens upregulate estrogen receptor beta expression and inhibit adrenocortical H295R cell proliferation. J Mol Endocrinol 35:245–56, 2005 doi:10.1677/jme.1.01806.
22. Bassett MH, Mayhew B, Rehman K, White PC, Mantero F, Arnaldi G, Stewart PM, Bujalska I, Rainey WE. Expression profiles for steroidogenic enzymes in adrenocortical disease. J Clin Endocrinol Metab 90:5446–55, 2005 doi:10.1210/jc.2005-0836.
23. Shigematsu K. Comparative studies between hormone contents and morphological appearances in human adrenal cortex—special reference to non-functioning tumors (adenoma and adenomatous nodule) and functioning adenoma. Acta Histochem Cytochem 15:386–400, 1982.
24. Omura M, Sasano H, Fujiwara T, Yamaguchi K, Nishikawa T. Unique cases of unilateral hyperaldosteronemia due to multiple adrenocortical micronodules, which can only be detected by selective adrenal venous sampling. Metabolism 51:350–5, 2002 doi:10.1053/meta.2002.30498.

Cytotechnology (2009) 60:161–164
DOI 10.1007/s10616-009-9229-5

BRIEF REPORT

Different expression levels of TNF receptors on the rheumatoid synovial macrophages derived from surgery and a synovectomy as detected by a new flow cytometric analysis

Hiroaki Ida · Toshiyuki Aramaki · Hideki Nakamura · Keita Fujikawa · Kazuhiko Arima · Mami Tamai · Makoto Kamachi · Katsuya Satoh · Tomoki Origuchi · Atsushi Kawakami · Itaru Furuichi · Yojiro Kawabe · Katsumi Eguchi

Received: 27 December 2008 / Accepted: 14 September 2009 / Published online: 26 September 2009

Abstract TNFα plays a crucial role in the pathogenesis of rheumatoid arthritis. It is very important to examine the expression of the TNF receptors, the ligand of TNFα. In this study, we developed a triple-color flow cytometric analysis using CD45 and CD14 monoclonal antibodies to simply detect the expression of the TNF receptors on the heterogeneous rheumatoid synovial cells. Using this system, we detected a higher population of macrophages and a greater TNF receptor expression on the synovial macrophages derived from a synovectomy in comparison to the findings obtained from knee joint replacement surgery.

Keywords Rheumatoid arthritis · Synovial cell · TNF receptor · Flow cytometry · Synovectomy · Macrophage

H. Ida (✉) · T. Aramaki · H. Nakamura · K. Fujikawa · K. Arima · M. Tamai · M. Kamachi · K. Satoh · A. Kawakami · K. Eguchi
First Department of Internal Medicine, Nagasaki University Hospital, Graduate School of Biomedical Sciences, Nagasaki University, 1-7-1 Sakamoto, Nagasaki 852-8501, Japan
e-mail: idah@net.nagasaki-u.ac.jp

T. Origuchi
Nagasaki University School of Health Sciences, Nagasaki, Japan

I. Furuichi · Y. Kawabe
NHO Ureshino Medical Center, Saga, Japan

Introduction

Rheumatoid arthritis (RA) is an autoimmune disease which is characterized by inflammatory synovitis and bone erosion (Feldmann et al. 1996a; Huber et al. 2006; Muller-Ladner et al. 2007; Schett 2008; Sweeney and Firestein 2004). Although the etiologies of RA have yet to be clearly defined, the persistence of autoreactive cells might lead to cytokine production (i.e., TNFα and IL-6). Recently, TNF blockers have also been used in patients with RA, and many patients have been reported to benefit from these agents (Feldmann and Maini 2001), thus suggesting that TNFα plays an important role in the pathogenesis of RA in patients. TNFα has the ability to bind two distinct TNF receptors, TNFR1 (TNFRSF1A) and TNFR2 (TNFRSF1B) (Baud and Karin 2001; Beyaert et al. 2002; MacEwan 2002; Wallach et al. 1999). The binding of TNFR1 triggers the release of the inhibitory protein silencer of death domains (SODD) and forms a receptor-proximal complex containing the adapter proteins. The engagement of TNF receptors results in the activation of two major transcription factors, nuclear factor κB (NF-κB) and c-Jun. These transcription factors induce the expression of genes that mediate diverse biological processes (Baud and Karin 2001; Beyaert et al. 2002; Chen and Goeddel 2002; MacEwan 2002; Wallach et al. 1999), especially in RA. For this reason, it is very important to examine the expression of TNF receptors on rheumatoid synovial cells.

The rheumatoid synovium contains a variety of cells, including macrophage-like cells (type A), fibroblast-like cells (type B), dendritic-like cells, and infiltrated lymphocytes (Feldmann et al. 1996b). These heterogeneous populations made it difficult to examine the pathogenesis of RA. In this study, we developed a new flow cytometric analysis in the synovial cells regarding the expression of surface molecules on each cell. Using this simple system, we detected a higher population of macrophages and a greater TNF receptor expression on the synovial macrophages derived from a synovectomy in comparison to those from knee joint replacement surgery.

Materials and methods

Cells

Synovial tissue specimens were obtained from patients with RA at the time of orthopedic surgery (knee joint replacement surgery or synovectomy) in the National Ureshino Hospital. Informed consent was obtained from all participating subjects, and the study was conducted in accordance with the human experimental guidelines of our institution. Synovial cells were isolated from the synovial tissues by an enzymatic digestion, as described previously (Yamasaki et al. 2002). Adherent synovial cells of at least four passages were used in this experiment as the cultured synovial cells. Before the analysis of the cultured adherent synovial cells, 0.5 mM EDTA solution with PBS was used to release the cells from the plastic plates. Trypsin–EDTA solution was not used, in order to avoid changes of the expression of surface molecules on the cells.

Monoclonal antibodies (mAb) and flow cytometry

PE-conjugated anti-human CD45, PC5-conjugated anti-human CD14, and PE-conjugated and PC5-conjugated control mAb (IgG1) were purchased from Beckmann Coulter (Hialeah, FL). FITC-conjugated anti-human TNFR1 and anti-human TNFR2 were purchased from R&D (Minneapolis, MN). FITC-conjugated anti-human control mAb (IgG1) were purchased from Beckmann Coulter. The triple-immunofluorescence analysis method has been described in detail elsewhere (Eguchi et al. 1989). The triple-immunofluorescence experiments were analyzed with a flow cytometer (Epics XL; Coulter Electronics, Hialeah, FL).

Results and discussion

We examined the two sources of the rheumatoid synovium which were derived from knee joint replacement surgery and a synovectomy. The disease activity of RA patients who were operated on for knee joint replacement should be low in comparison to that of patients who received a synovectomy, because the knee joint replacement is performed in the majority of RA patients whose knee joints were destroyed after long-time therapy. To elucidate the real status of the rheumatoid synovium, it would be useful to use the cells from the active inflammatory phase in the experiments. This is the reason why synovial cells derived from both knee joint replacement surgery (Fig. 1a) and a synovectomy (Fig. 1b) were used and then the cell population and the expression of TNF receptors were compared between the two sources of synovial cells in this experiment. Figure 1 shows that the main population would be from the macrophage region (CD45+CD14+) in the freshly isolated synovial cells derived from both knee joint replacement surgery and a synovectomy. A higher population of macrophages was detected in the cells from a synovectomy in comparison to those obtained from knee joint replacement surgery (61.9 and 45.8%, respectively). After the isolated synovial cells were cultured for a long time (at least 4 times passages), the percentage of macrophage-like cells was decreased; in contrast, the percentage of fibroblast-like cells was increased in the synovial cells derived from both knee joint replacement surgery and a synovectomy. Regarding the expression of TNF receptors, a small percentage of TNFR1 expressed cells was detected in both the macrophage and fibroblast cell regions in the synovial cells derived from both knee joint replacement surgery and a synovectomy. On the other hand, the TNFR2 expression on the macrophage-like cells was sufficiently detected, whereas no TNFR2 expression was observed on the fibroblast-like cells in the synovial cells derived from both knee joint replacement surgery and a synovectomy (Fig. 1). Interestingly, the expression of both TNFR1 and TNFR2 on the synovial macrophages derived from a synovectomy was higher

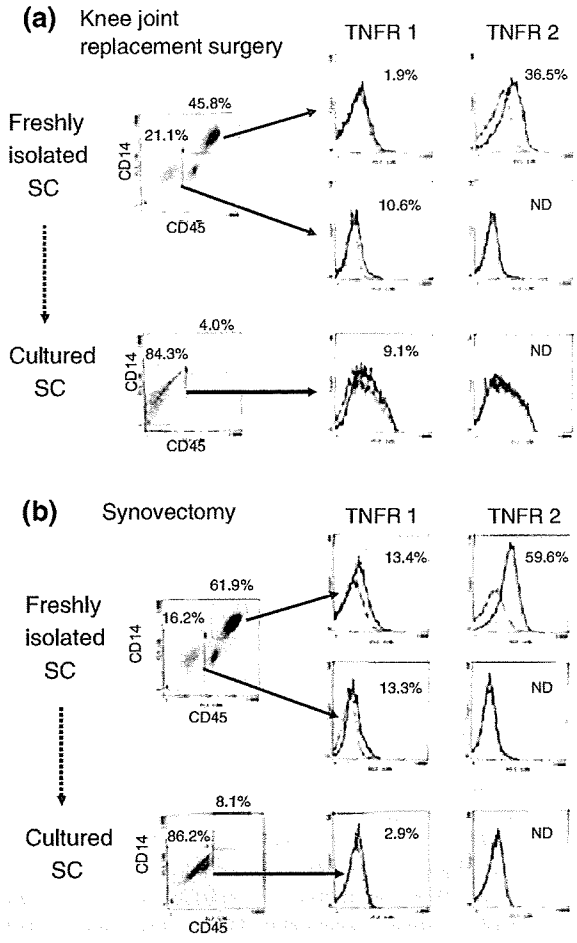

Fig. 1 Altered TNF receptor expression on synovial cells after long-time culture. A triple-color flow cytometric analysis of TNF receptors in the synovial cells derived from knee joint replacement surgery (**a**) and a synovectomy (**b**). Both cells were analyzed for the surface expression of TNF receptors (*TNFR1* and *TNFR2*) on the CD14+CD45+ population or CD14−CD45− population. In the *upper panel* (**a** and **b**), the synovial cells were derived from the freshly isolated cells. In the *lower panel* (**a** and **b**), the synovial cells are derived from the long-time cultured cells. In each histogram, the background fluorescence is recorded with a thin line, and the thick-lined histogram quantifies the expression of the indicated molecules (% = percentage of positive expression of each of the molecules). One of four representative experiments is shown. *SC* synovial cell, *ND* not detected

than that from knee joint replacement surgery (13.4 and 1.9% in TNFR1, 59.6 and 36.5% in TNFR2, respectively), thus suggesting that synovial macrophages from a synovectomy may be more highly activated than those from knee joint replacement surgery, while also reflecting an increased disease activity.

Rheumatoid synovial tissue contains macrophage-like cells (type A), fibroblast-like cells (type B), dendritic-like cells, and infiltrated lymphocytes, demonstrating that these heterogeneous cells would constitute the RA inflammatory synovium (Feldmann et al. 1996b; Karouzakis et al. 2006; Muller-Ladner et al. 2007). We previously reported apoptosis (Kawakami et al. 1999, 2004; Miyashita et al. 2003, 2004; Tamai et al. 2006), cell differentiation (Yamasaki et al. 2004), cell proliferation (Eguchi et al. 1992; Migita et al. 2000, 2001), signal transduction (Yamasaki et al. 2001, 2002), sensitivity to drugs (Migita et al. 2004), and protein expression of the rheumatoid synovial cells (Honda et al. 2001; Tanaka et al. 2004) using the long-time cultured synovial cells derived from the knee joint replacement surgery. As the cell population and the expression of TNF receptors both dramatically changed in the synovial cells derived from both surgery and a synovectomy after long-term cultures (Fig. 1a, b), it would be difficult to evaluate the real function of the rheumatoid synovial cells using such long-term cultured cells. However, we had no chance to use these long-term cultured synovial cells in our previous experiments, because a large number of such cells are needed to perform the assays, and the necessary amount of cells was just not available. If we use this simple flow cytometric method, we can independently evaluate the expression of surface molecules on each cell type derived from the freshly isolated synovial cells, and thus making it possible to elucidate the present status of the RA synovium.

In summary, we developed a simple detection system, which was a triple-color flow cytometric analysis, using CD45 and CD14 monoclonal antibodies on rheumatoid synovial cells. Using this system, we detected a higher population of macrophages and a greater TNF receptor expression on the synovial macrophages derived from a synovectomy in comparison to that obtained during knee joint replacement surgery. This flow cytometric analysis is therefore considered to reflect the real status of the disease using rheumatoid synovial cells, especially those derived from a synovectomy.

Acknowledgments This research was supported in part by a Grant-in-aid from the Ministry of Health, Labor, and Welfare, Japan (to HI). HI, MK, and TO are fellows of the Japanese Society of Internal Medicine.

References

Baud V, Karin M (2001) Signal transduction by tumor necrosis factor and its relatives. Trends Cell Biol 11:372–377

Beyaert R, Van Loo G, Heyninck K, Vandenabeele P (2002) Signaling to gene activation and cell death by tumor necrosis factor receptors and Fas. Int Rev Cytol 214: 225–272

Chen G, Goeddel DV (2002) TNF-R1 signaling: a beautiful pathway. Science 296:1634–1635

Eguchi K, Ueki Y, Shimomura C, Otsubo T, Nakao H, Migita K et al (1989) Increment in the Ta1+ cells in the peripheral blood and thyroid tissue of patients with Graves' disease. J Immunol 142:4233–4240

Eguchi K, Migita K, Nakashima M, Ida H, Terada K, Sakai M et al (1992) Fibroblast growth factors released by wounded endothelial cells stimulate proliferation of synovial cells. J Rheumatol 19:1925–1932

Feldmann M, Maini RN (2001) Anti-TNF alpha therapy of rheumatoid arthritis: what have we learned? Annu Rev Immunol 19:163–196

Feldmann M, Brennan FM, Maini RN (1996a) Rheumatoid arthritis. Cell 85:307–310

Feldmann M, Brennan FM, Maini RN (1996b) Role of cytokines in rheumatoid arthritis. Annu Rev Immunol 14:397–440

Honda S, Migita K, Hirai Y, Origuchi T, Yamasaki S, Kamachi M et al (2001) Expression of membrane-type 1 matrix metalloproteinase in rheumatoid synovial cells. Clin Exp Immunol 126:131–136

Huber LC, Distler O, Tarner I, Gay RE, Gay S, Pap T (2006) Synovial fibroblasts: key players in rheumatoid arthritis. Rheumatology (Oxford) 45:669–675

Karouzakis E, Neidhart M, Gay RE, Gay S (2006) Molecular and cellular basis of rheumatoid joint destruction. Immunol Lett 106:8–13

Kawakami A, Nakashima T, Sakai H, Hida A, Urayama S, Yamasaki S et al (1999) Regulation of synovial cell apoptosis by proteasome inhibitor. Arthritis Rheum 42:2440–2448

Kawakami A, Urayama S, Yamasaki S, Hida A, Miyashita T, Kamachi M et al (2004) Anti-apoptogenic function of TGFbeta1 for human synovial cells: TGFbeta1 protects cultured synovial cells from mitochondrial perturbation induced by several apoptogenic stimuli. Ann Rheum Dis 63:95–97

MacEwan DJ (2002) TNF receptor subtype signalling: differences and cellular consequences. Cell Signal 14:477–492

Migita K, Honda S, Yamasaki S, Hirai Y, Fukuda T, Aoyagi T et al (2000) Regulation of rheumatoid synovial cell growth by ceramide. Biochem Biophys Res Commun 269:70–75

Migita K, Tanaka F, Yamasaki S, Shibatomi K, Ida H, Kawakami A et al (2001) Regulation of rheumatoid synoviocyte proliferation by endogenous p53 induction. Clin Exp Immunol 126:334–338

Migita K, Miyashita T, Ishibashi H, Maeda Y, Nakamura M, Yatsuhashi H et al (2004) Suppressive effect of leflunomide metabolite (A771726) on metalloproteinase production in IL-1beta stimulated rheumatoid synovial fibroblasts. Clin Exp Immunol 137:612–616

Miyashita T, Kawakami A, Tamai M, Izumi Y, Mingguo H, Tanaka F et al (2003) Akt is an endogenous inhibitor toward tumor necrosis factor-related apoptosis inducing ligand-mediated apoptosis in rheumatoid synovial cells. Biochem Biophys Res Commun 312:397–404

Miyashita T, Kawakami A, Nakashima T, Yamasaki S, Tamai M, Tanaka F et al (2004) Osteoprotegerin (OPG) acts as an endogenous decoy receptor in tumour necrosis factor-related apoptosis-inducing ligand (TRAIL)-mediated apoptosis of fibroblast-like synovial cells. Clin Exp Immunol 137:430–436

Muller-Ladner U, Ospelt C, Gay S, Distler O, Pap T (2007) Cells of the synovium in rheumatoid arthritis. Synovial fibroblasts. Arthritis Res Ther 9:223

Schett G (2008) Review: immune cells and mediators of inflammatory arthritis. Autoimmunity 41:224–229

Sweeney SE, Firestein GS (2004) Rheumatoid arthritis: regulation of synovial inflammation. Int J Biochem Cell Biol 36:372–378

Tamai M, Kawakami A, Tanaka F, Miyashita T, Nakamura H, Iwanaga N et al (2006) Significant inhibition of TRAIL-mediated fibroblast-like synovial cell apoptosis by IFN-gamma through JAK/STAT pathway by translational regulation. J Lab Clin Med 147:182–190

Tanaka F, Migita K, Kawabe Y, Aoyagi T, Ida H, Kawakami A et al (2004) Interleukin-18 induces serum amyloid A (SAA) protein production from rheumatoid synovial fibroblasts. Life Sci 74:1671–1679

Wallach D, Varfolomeev EE, Malinin NL, Goltsev YV, Kovalenko AV, Boldin MP (1999) Tumor necrosis factor receptor and Fas signaling mechanisms. Annu Rev Immunol 17:331–367

Yamasaki S, Kawakami A, Nakashima T, Nakamura H, Kamachi M, Honda S et al (2001) Importance of NF-kappaB in rheumatoid synovial tissues: in situ NF-kappaB expression and in vitro study using cultured synovial cells. Ann Rheum Dis 60:678–684

Yamasaki S, Nakashima T, Kawakami A, Miyashita T, Ida H, Migita K et al (2002) Functional changes in rheumatoid fibroblast-like synovial cells through activation of peroxisome proliferator-activated receptor gamma-mediated signalling pathway. Clin Exp Immunol 129:379–384

Yamasaki S, Nakashima T, Kawakami A, Miyashita T, Tanaka F, Ida H et al (2004) Cytokines regulate fibroblast-like synovial cell differentiation to adipocyte-like cells. Rheumatology (Oxford) 43:448–452

Original Research Article

Dementia
and Geriatric
Cognitive Disorders

Dement Geriatr Cogn Disord 2009;28:550–557
DOI: 10.1159/000254842

Accepted: October 7, 2009
Published online: December 30, 2009

Familial Creutzfeldt-Jakob Disease with a V180I Mutation: Comparative Analysis with Pathological Findings and Diffusion-Weighted Images

Kazuo Mutsukura[a] Katsuya Satoh[a] Susumu Shirabe[c] Itsuro Tomita[d]
Takayasu Fukutome[e] Minoru Morikawa[b] Masachika Iseki[f] Kensuke Sasaki[g]
Yusei Shiaga[h] Tetsuyuki Kitamoto[i] Katsumi Eguchi[a]

[a]First Department of Internal Medicine and [b]Department of Radiology and Radiation Biology, Graduate School of Biomedical Sciences, Nagasaki University, and [c]Organization of Rural Medicine and Residency Education, Nagasaki University Hospital, Nagasaki, [d]Nagasaki Kita Hospital, Togitsu, [e]Kawatana National Hospital, Kawatana, [f]Pathology, Sasebo Kyosai Hospital, Sasebo, [g]Department of Neuropathology, Neurological Institute, Graduate School of Medical Sciences, Kyushu University, Fukuoka, and [h]Aoba Neurosurgery and [i]Department of Neurological Science, Graduate Medical School of Tohoku University, Sendai, Japan

Key Words
Creutzfeldt-Jakob disease · Diffusion-weighted imaging · Magnetic resonance spectroscopy · Single-photon emission computed tomography · Brain biopsy

Abstract
Background: Diffusion-weighted imaging (DWI) has been reported to be a useful technique for diagnosing Creutzfeldt-Jakob disease (CJD). The present study reported DWI results in cases of familial CJD with a V180I mutation (CJD180) in the prion protein gene as well as neurological findings. ***Methods:*** A retrospective analysis of 3 patients with V180I was performed. Cerebrospinal fluid (CSF) analysis, brain MRI, single-photon emission computed tomography (SPECT), and magnetic resonance spectroscopy (MRS) were included. CSF was analyzed for biochemical markers, and each patient underwent brain MRI, SPECT, and MRS analysis. A brain biopsy from the frontal cortex, which corresponded to the area of increased DWI signals, was utilized for neuropathological analysis. ***Results:*** CSF analysis results revealed elevated total tau protein and the absence of 14-3-3 protein, as well as decreased concentrations of neuron-specific enolase, S100 protein, and prostaglandin E_2. All patients presented with unique MRI features. Brain biopsy showed severe spongiform morphology, but comparatively preserved neurons and mild astrocytic gliosis. Accumulations of PrP^{Sc} were not detected using the 3F4 antibody, and microglial activation was subtle. SPECT revealed hypoperfusion throughout both hemispheres. MRS revealed a reduced N-acetyl aspartate/creatine ratio. ***Conclusion:*** Results from this study suggested that increased DWI signals could reflect severe spongiform changes in CJD180 patients.

Introduction

Creutzfeldt-Jakob disease (CJD) is a transmissible spongiform encephalopathy associated with the accumulation of abnormal prion protein. The disease has been classified into sporadic, familial, and infectious subtypes.

KARGER
Fax +41 61 306 12 34
E-Mail karger@karger.ch
www.karger.com

1420–8008/09/0286–0550$26.00/0

Accessible online at:
www.karger.com/dem

Katsuya Satoh
First Department of Internal Medicine, Graduate School of Biomedical Science
Nagasaki University, 1-7-1 Sakamoto
Nagasaki 852-8501 (Japan)
Tel. +81 95 819 7269, Fax +81 95 819 7270, E-Mail f1537@cc.nagasaki-u.ac.jp

Familial CJD (fCJD) comprises approximately 15% of all human prion disease, and is a result of point mutations or insertions in the prion protein gene (PRNP). To date, 30 subtypes of the familial form have been determined, of which 24 are due to mutations and 6 are a result of insertions. CJD, with a causative point mutation of valine to isoleucine at codon 180 (V180I) in the PRNP, is a rare type of fCJD, with only 2 cases reported from Europe [1, 2]. However, this mutation is recognized as the most common cause of fCJD in Japan.

Jin et al. [3] reported that CJD patients with the V180I (CJD180) mutation exhibit characteristic clinical features, and that the clinical and neuroradiological findings of CJD180 patients vary from classical CJD patients in: (1) older onset age, (2) slower disease progression, (3) unique clinical symptoms, such as greater cortical dysfunction, which is less frequent in sporadic CJD (sCJD) patients, with none of the visual or cerebellar symptoms that are frequently observed in sCJD patients, (4) reduced rate of brain-specific proteins, such as neuron-specific enolase (NSE) and 14-3-3 protein, in cerebrospinal fluid (CSF) samples, and (5) the lack of a periodic sharp discharge (PSD) in the electroencephalogram (EEG) throughout the course of disease.

Diffusion-weighted imaging (DWI) may be useful in the premortem diagnosis of sCJD, and recent reports have suggested its usefulness in fCJD cases. Jin et al. [3] reported that diffuse cortical high-intensity DWI signals are a characteristic feature of CJD180. The exact mechanisms responsible for high-intensity signals on DWI have not yet been established. Many reports have described the relationship between autopsy and DWI findings. However, brain biopsy is rarely performed, and autopsy results are not always consistent with lesions revealed by DWI abnormalities and do not always reflect the pathogenesis of DWI abnormalities. This confirms the importance of reporting and analyzing biopsy cases for neuropathology. Neuropathological findings in CJD180 patients have revealed significant spongiform changes throughout all cell layers of the gray matter, and neuronal numbers were relatively preserved, with very little abnormal prion protein expression.

A detailed analysis of the pathogenesis, which was reflected in abnormal pathological features in DWI-based neuroimaging and biochemical markers of CSF, was performed. In addition, 3 CJD180 patients were studied using MRI, magnetic resonance spectroscopy (MRS), and single photon emission-computed tomography (SPECT).

Materials and Methods

Subjects

Case 1. A 70-year-old woman was admitted with progressive memory loss. Approximately 1 year prior to admission, neighbors began noticing that the patient exhibited amnesia. Six months later, the patient began to forget things and became disoriented. Finally, the patient was unable to walk without support and was admitted to hospital. DWI demonstrated diffuse bilateral high-intensity signals in the cerebral cortex, caudate nucleus and putamen, but was predominant in the left hemisphere. The patient was right-handed. Therefore, a brain biopsy from the right frontal cortex was performed. The brain biopsy area corresponded to the region of increased DWI signals. Following CJD diagnosis, she was transferred to our university hospital. Upon admission, the patient was bedridden and exhibited myoclonic jerks and startle reactions. Muscle rigidity was present in all extremities, and deep tendon reflexes were exaggerated. CSF analysis was normal, except for negative 14-3-3 protein and elevated total tau (t-tau) protein. The patient exhibited no PSD on EEG. Genetic analysis revealed a V180I point mutation, leading to the diagnosis of fCJD. She was not able to follow simple commands and to move to the bed alone during the 12-month period after onset.

Case 2. A 67-year-old woman was admitted with a 6-month history of progressive aphasia. The past medical and family histories were unremarkable apart from cholecystectomy 17 years earlier. Upon examination, the patient was disoriented and forgetful of recent events. She did not exhibit cerebellar ataxia or myoclonus. The patient had been diagnosed with dementia of Alzheimer's type (DAT) in another hospital, but the symptoms progressed more rapidly than typical DAT. She was able to follow simple commands, but gradually lost the ability to walk.

T_2-weighted imaging (T2WI) and DWI revealed increased signals in the bilateral tempoparietal cortex, predominantly in the left hemisphere. EEG revealed no PSD. Detection of the codon 180 point mutation in PRNP confirmed the diagnosis of fCJD.

The patient gradually developed speech difficulties over a 6-month period and was not able to speak by 7 months after onset. She could not follow simple commands and move to the bed alone during the 12-month period after onset.

Case 3. A 74-year-old man became disoriented while returning home from shops to which he was accustomed to traveling back and forth. The patient was unable to walk unassisted, developed urinary incontinence and began to exhibit progressive memory disturbances 1 month later. He was admitted to our hospital, and DWI abnormalities were noted. A double mutation at codons 180 and 232 (Met/Arg) of PRNP was detected, leading to a diagnosis of fCJD. The patient gradually developed speech difficulties by 4 months after onset and was unable to speak by 6 months after onset. The patient could not follow simple commands or move to the bed unassisted by 12 months after onset.

During World War II, on August 9, 1945, the city of Nagasaki was destroyed by an atomic bomb, killing tens of thousands of people. As a result of this tragedy, detailed family histories of these CJD patients remain unknown.

Social and personal conduct disorders, such as frontotemporal lobar degeneration (FTLD), and behavioral and psychological symptoms of dementia, such as DAT, were not observed in the 3 CJD180 patients. However, depressive symptoms and sleep dis-

turbances were noted at onset. The patients did not exhibit akinetic mutism during their lifetime.

Biochemical Analysis of CSF Samples

CSF samples from all 3 patients were analyzed by ELISA for t-tau protein, phosphorylated tau (p-tau) protein, S100 protein, NSE, and prostaglandin E_2 (PGE_2) concentrations, as well as by Western blot analysis for 14-3-3 protein expression. A polyclonal antibody specific for the β-isoform of 14-3-3 protein (sc-639; Santa Cruz, Calif., USA) was used in combination with an enhanced chemiluminescence detection kit (Amersham Buchler, Braunschweig, Germany). ELISAs were performed according to the manufacturer's instructions, using an identical standard in all experiments.

Brain MRI Procedure

MRI was performed on all subjects using a 1.5-tesla magnetic resonance unit (General Electric Medical System, Milwaukee, Wisc., USA) with T_1-weighted imaging (T1WI) [repetition time (TR) = 400 ms, echo time (TE) = 9/Fr ms], T2WI (TR = 3,000 ms, TE = 97 ms), fluid attenuation inversion recovery (TR = 8,002 ms, TE = 104/ms), and DWI sequences of 5-mm slice thickness. The acquired data were analyzed using Digital Imaging and Communications in Medicine (DICOM) format.

SPECT Image Analysis Using eZIS and N-Isopropyl-p-[^{123}I]-Iodoamphetamine

SPECT was performed using ^{99m}Tc-ethyl cysteinate dimer (^{99m}Tc-ECD) and N-isopropyl-*p*-[^{123}I]-iodoamphetamine (^{123}I-IMP) as a tracer in all subjects. Obtained images were anatomically standardized with an original ^{99m}Tc-ECD template using the easy *Z*-score imaging system (eZIS) established by Matsuda et al. [4].

Magnetic Resonance Spectroscopic Analysis

Single-voxel ^{1}H-MRS was performed. Spectra were acquired from an 8-ml cubic volume of interest centered on the right cerebral cortex.

Neuropathological Investigation

The right frontal lobe brain biopsy from case 1 corresponded with increased DWI signals. The time interval between brain biopsy and DWI was 1 day.

Formalin-fixed, paraffin-embedded sections of brain biopsy tissue were subjected to histological analyses, including hematoxylin-eosin (HE) staining and PrP^{Sc} immunohistochemistry with 3F4 monoclonal antibody. Glial activation (astrocytic gliosis and microglia activation) was assessed by immunohistochemistry on tissue sections using S100 protein and CD68. The neuropathological findings (HE staining, S100 protein, CD68, and 3F4 immunohistochemistry) were assessed in biopsy tissue from case 1 and compared with autopsy tissue from 4 typical sCJD cases.

Statistical Analysis

Comparisons of clinical symptoms between the present cases, 7 cases described in previous reports, and pooled data from sCJD patients were performed using the χ^2 test and Student's t test. The Medical Ethics Committee of Nagasaki University School of Medicine approved this study, and the participants provided written informed consent.

Results

Clinical Findings in CJD180 Patients

Clinical features from the 3 cases are summarized in table 1.

The age at onset was 69 ± 1.41 years in the 3 CJD180 patients. When the 4 CJD180 patients described in previous reports were combined with this analysis, the age at onset of the 7 CJD180 patients was 70.3 ± 3.9 years. There was no statistically significant difference in age at onset between the present CJD180 patients and the previously described sCJD patients (65.3 ± 11.6 years old; n = 128).

Appearance of myoclonic jerk from disease onset was 5.33 ± 0.93 months in the present 3 CJD180 patients, and 8.0 ± 4.5 months in all 7 CJD180 patients (including 4 previously described patients). Myoclonic jerk was identified in all cases, but the duration to appearance was longer in CJD180 patients compared with sCJD patients (2.7 ± 2.4 months). The myoclonic jerks were less remarkable in the present patients compared with the sCJD patients, and the myoclonic jerks of all CJD180 patients exhibited a similar frequency to Parkinson's disease tremors (5–9 Hz).

Time to appearance of akinetic mutism from disease onset was 12.3 ± 4.50 months in the present 3 CJD180 patients and 11.7 ± 3.34 months in all 7 CJD180 patients (including 4 previously described patients). The time to appearance of akinetic mutism was longer in CJD180 patients compared with sCJD patients ($p < 0.01$). Survival time of the present 3 CJD180 patients was 30.3 ± 4.78 months.

Biochemical Analysis of CSF

The biochemical markers used for CSF analysis are listed in table 1.

CSF from all patients was negative for 14-3-3 protein (present and previously described cases). 14-3-3 protein was detected in 87.7% of the sCJD patients. Therefore, 14-3-3 protein expression in CSF was not used as a diagnostic marker for CJD180.

In the patients from this study, t-tau protein titers were greater than the cut-off level (1,300 pg/ml), but much less than in the sCJD cases (5,689 ± 169 pg/ml; n = 128; data not shown). NSE concentrations in all 3 cases were less than the cut-off value (35 ng/ml), but greater than the concentrations in individuals with neurodegenerative disorders (10.35 ± 4.35 ng/nl; n = 100). S100 protein and PGE_2 protein concentrations were below the detection thresholds.

Table 1. Profiles of the 3 cases with CJD180

	Our cases			Previously reported[1]	
	case 1	case 2	case 3	CJD180	sCJD
Age/sex	70/F	67/F	70/M	70.3 ± 3.9	65.3 ± 11.6
Family history	–	–	–	–	–
Myoclonic jerk, months	6	6	4	8.0 ± 4.5	2.7 ± 2.4
Visual symptoms	–	–	–	0% (0/4)	24% (23/96)
Cerebellar symptoms	–	–	–	0% (0/4)	12.5% (12/96)
Akinetic mutism, months	12	18	7	11.3 ± 2.2	3.5 ± 2.8
Total tau, pg/ml	3,811	2,325	3,675	NE	89.6% (86/96)
Phosphorylated tau, pg/ml	39.4	40.8	36.1	NE	NE
NSE, ng/ml	34	22	13	50% (2/4)	72.7% (48/66)
S100 protein, ng/ml	0.23	0.35	0.13	NE	NE
14-3-3 protein	–	–	–	0%	87.7% (57/65)
PSD	–	–	–	0%	94% (110/116)
Codon 129 in PRNP	M/M	M/M	M/M	MM 40%; MV60%	MM 91%; MV 9%
Codon 219 in PRNP	E/E	E/E	E/E	E/E 100%	E/E 92%; E/K8%
Type of PrP^{Sc}	type 1+2	NE	NE	NE	type 1 or type 2

Range of t-tau protein levels: 800–15,000 ng/ml, CJD with values >1,300 pg/ml.

Range of p-tau protein levels: 8–120 ng/ml.

Range of NSE levels: 2–200 ng/ml, CJD with values >35 ng/ml.

Range of S100 protein levels: 0.001–25 ng/ml, CJD with values >2.2 ng/ml.

We analyzed the cutoff data of t-tau protein, NSE and S100 protein of CSF among 128 CJD patients and 100 non-CJD patients (DAT, vascular dementia, Pick's disease, Parkinson's disease, corticobasal degeneration, Huntington's disease, frontotemporal dementia, progressive supranuclear palsy, mild cognitive impairment, amyotrophic lateral sclerosis, temporal epilepsy, limbic encephalopathy, paraneoplastic cerebellar degeneration/Lambert-Eaton myasthenic syndrome, MELAS and encephalopathy due to unknown etiology). The most appropriate cutoff levels of biomarkers (t-tau protein, NSE and S100 protein of CSF) in CJD patients were evaluated using the receiver-operating characteristics curve method. The sensitivities for t-tau protein, 14-3-3 protein, NSE and S100 protein of CSF in classical CJD patients (n = 128) were 95.9, 88.7, 81.5 and 33.1%, respectively (data not shown).

In all 3 patients, the polymorphism in PRNP at codon 129 was homozygous for methionine (M/M), while the polymorphism in PRNP at codon 219 was homozygous for glutamic acid (E/E). NE = Not examined; M = methionine; V = valine; K = lysine; E = glutamic acid.

[1] As previously reported by Jin et al. [3], the average level of t-tau protein of classical CJD patients (n = 128) was 5,689 ± 169 pg/ml (average ± 1 SD).

Neuroimaging (MRI, MRS, SPECT)

According to the MRI results, all cases demonstrated a wide range of cerebral cortical ribbons, which were depicted as low-intensity areas in the bilateral putamen, caudate head, and cerebral cortex by T1WI, and as high-intensity areas by T2WI, fluid attenuation inversion recovery, and DWI. The cortical lesion was not always symmetric (cases 1 and 2). Basal ganglia lesions were detected, and the caudate head was detected in all cases (fig. 1). The cerebellum and brain stem were not abnormal.

MRS revealed decreased N-acetyl aspartate (NAA)/creatine (Cr) and choline (Cho)/Cr ratios in the cerebral cortices of all patients (table 2), whereas there were no changes in myoinositol (MI) levels (fig. 2). SPECT images from case 2 revealed a widespread decreased perfusion in both cerebral hemispheres, in particular the left temporal cortex (table 2). Highly insensitive DWI regions were observed throughout the cerebral cortex in the CJD180 cases and were similar to the smaller volume area observed on SPECT (fig. 2). Regional cerebral blood flow in the cerebral cortex was less in the CJD180 cases than in the sCJD cases.

Diagnosis of CJD

The characteristic clinical finding in the 3 CJD180 patients was progressive dementia and memory disturbance; the time course of the progressive dementia in the 3 CJD180 patients was different from that of DAT or FTLD, and was also different from typical sCJD patients. The psychiatric findings in the 3 CJD180 patients includ-

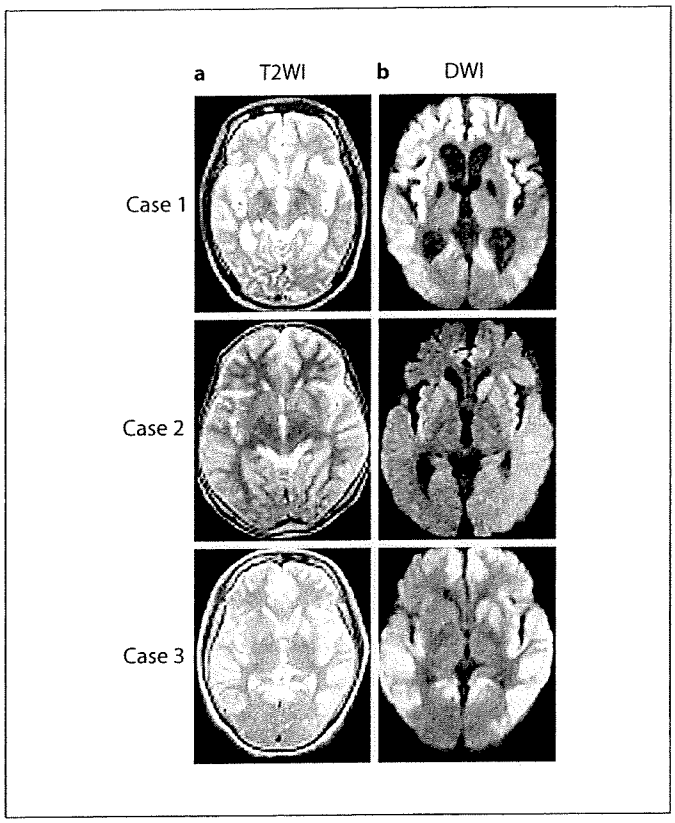

Fig. 1. Axial T_2- (**a**) and diffusion-weighted (**b**) MR images from the 3 CJD cases with the V180I mutation, revealing extensive cortical hyperintensity lesions. Hyperintense signals in the bilateral caudate nucleus and putamen are also demonstrated, but these are subtle compared with the cortical lesions. Medial regions of the occipital lobes are not involved.

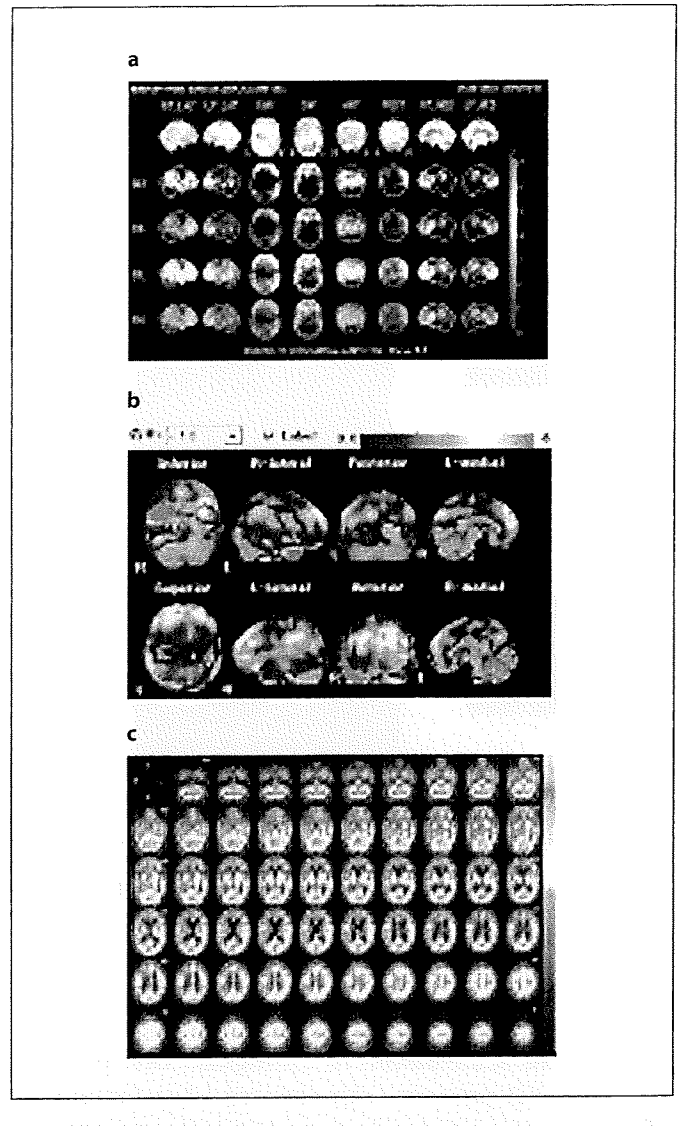

Fig. 2. SPECT analysis in case 1 (CJD180). **a** ^{123}I-IMP SPECT demonstrated decreased uptake. **b** eZIS analysis in SPECT performed using ^{99m}Tc-ECD. **c** 3DSRT analysis in SPECT performed using ^{99m}Tc-ECD.

Color version available online

ed depression and sleep disturbance, but disinhibition and asocial behavior were not determined in FTLD of the 3 CJD180 cases. In addition, behavioral and psychological symptoms of dementia in DAT were not recognized in the 3 CJD180 cases.

The 3 CJD180 patients were misdiagnosed with DAT. CSF samples were analyzed from 100 patients with various neurodegenerative disorders using Western blot to detect 14-3-3 protein, t-tau protein, and p-tau protein expressions. t-tau protein concentration in CSF of CJD patients was >1,200 pg/ml. However, the level of t-tau protein in CSF of neurodegenerative disorder patients was 200–500 pg/ml, and the level of t-tau protein from CSF of DAT patients was 400–1,400 pg/ml. Elevated t-tau protein was also detected in 3 patients from the non-CJD group. Elevated t-tau protein levels were observed in 2 patients with DAT and in 1 patient with cerebrovascular

Table 2. MRS in the 3 cases with CJD180 and 4 cases with sCJD

	Case 1	Case 2	Case 3	sCJD (n = 4)
NAA/Cr	0.79	1.1	1.3	1.83 ± 0.20
Cho/Cr	1.18	1.02	0.91	1.49 ± 0.20
MI	30	28	11	<30

sCJD (n = 4) patients were definite cases and the molecular type of the abnormal prion protein in sCJD cases was type 2 on Parchi's classification [6].

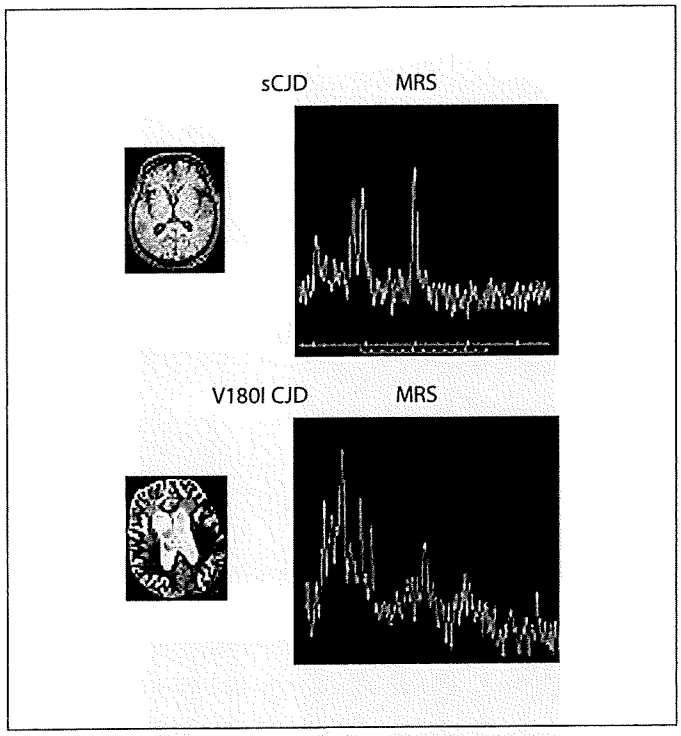

Fig. 3. ^{1}H-MRS in case 1 exhibits decreased cortical gray matter NAA/Cr.

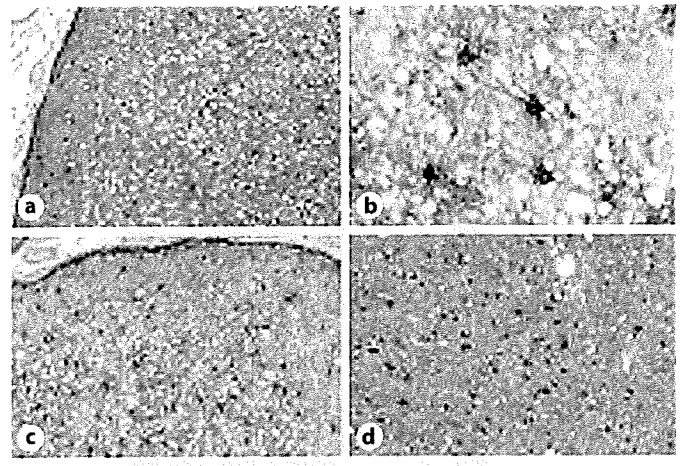

Fig. 4. Pathological findings in the right frontal lobe of case 1 reveal severe spongiform changes and neuronal loss. However, astrocytic gliosis, accumulation of PrP^{Sc}, and microglial activation are less apparent in the cerebral cortex. **a** HE staining. **b** CD68 staining. **c** S100b protein staining (×10). **d** S100b protein staining (×200).

disease in the acute phase. To distinguish CJD patients from non-CJD patients with elevated t-tau protein in CSF, the ratio of p-tau and t-tau proteins was compared. The p-/t-tau ratio was significantly greater in DAT patients compared with CJD patients. Some diseases revealed >2,000 pg/ml t-tau protein in the CSF of CJD patients. When it was difficult to distinguish CJD from DAT patients, the ratio of p-tau and t-tau proteins was compared.

The highest level of t-tau protein in the FTLD patients was 670 pg/ml, and there were no FTLD patients with CSF values >1,000 pg/ml t-tau protein, which was consistent with previous reports [5]. Results from CSF analysis, clinical disease course, and the neuroradiological findings in the V180I CJD patients varied between the DAT and FTLD patients.

Neuropathology

HE staining revealed severe spongiform changes in the cerebral cortex, which were more moderate in the CJD180 patients compared with the sCJD cases. The CJD180 patients exhibited a relatively limited neuronal loss compared with the sCJD patients (fig. 4a).

Immunostaining with 3F4 antibody was not detected in 1 patient (case 1), but all control cases of sCJD expressed 3F4 protein. CD68 expression was positive, but the number of CD68-positive microglia in the present sCJD cases was greater than in the CJD180 patients (fig. 4b). S100 immunohistochemistry demonstrated mild astrocytic gliosis in the CJD180 patients. However, 2 sCJD (early stage and middle stage) and 2 late-stage patients exhibited severe and moderate astrocytic gliosis, respectively (fig. 4c, d).

Typing of Protease-Resistant Prion Protein

According to Western blot analysis, the abnormal prion protein in the CJD180 cases was type 2 according to Parchi's classification [6].

Discussion

Neuropathological examination of tissue biopsies from case 1 demonstrated an unusual presentation compared with the biopsy sections from sCJD cases. First, all cell layers of the gray matter exhibited marked spongiform changes. Second, neuronal numbers were relatively preserved. Third, no abnormal prion protein expression was detected. Fourth, microglial activation was subtle. These results were consistent with the unique characterizations from previous reports [7–9].

Table 3. Neuropathological findings in 1 case with CJD180 (case 1) and 4 cases with sCJD

	CJD180 case 1	sCJD case 1	sCJD case 2	sCJD case 3	sCJD case 4
Neuronal loss	+	+	+	+++	+++
Astrocytic gliosis	+	++	++	+	+
Spongiform change	+++	++	++	+	+
Microglia activation	+	+++	++	++	++
PrP deposition	–	++	++	+++	++

Spongiform change and neuronal loss are described as absent (–), mild (+), moderate (++), and severe (+++) on HE sections.

Astrocytosis is described as absent (–), mild (+), moderate (++), and severe (+++) on sections labeled immunohistochemically with an anti-S100 antibody (polyclonal, DAKO, Glostrup, Denmark) or anti-prion protein antibody (monoclonal, clone 3F4, Senetek, Maryland Heights, Mo., USA).

Degree of prion protein deposition is described as absent (–), mild (+), moderate (++), and strong (+++) on sections labeled immunohistochemically with an anti-prion protein antibody (monoclonal, clone 3F4, DAKO, Japan).

Microglia activation (the number of CD68-positive microglia) is described as follows: no staining (–), slightly staining (+), moderate staining (++), and strong staining (+++).

More than 30 CJD patients have undergone brain biopsies, but only 3 reports [10–12] discussed the correlation between neuropathological and DWI findings in brain biopsy tissue. In other studies, brain biopsies were used only as a diagnostic method to rule out progressive dementia.

Heinemann et al. [10] suggested that the correlation between DWI and neuropathological findings in brain biopsies could be a result of neuronal loss and spongiform changes. Spongiform neuronal degeneration was demonstrated to underlie the increased DWI signals in sCJD patients as shown by Kim et al. [11]. In addition, See et al. [12] suggested that fluid accumulation within cytoplasmic vacuoles of the neuropil, or astrogliosis, contributes to a restricted diffusion range that underlies DWI abnormalities. Microglial activation has been suggested as another possible cause of DWI abnormalities. A relationship between DWI abnormalities and accumulation of PrP^{Sc} has been suggested as a possible causative mechanism [6, 13]. Results from the present study demonstrated very low abnormal prion protein expression. These results suggest that there is not a strong relationship between DWI abnormalities and PrP^{Sc} accumulation.

It is difficult to determine the mechanisms underlying DWI abnormalities based on results from a single brain biopsy. Although the present study utilized single brain biopsies, pathological analyses clearly revealed pathological findings in the sCJD cases (table 3). Nevertheless, the mechanism underlying the DWI abnormalities was assumed to be a result of severe spongiform changes as revealed by neuropathological findings.

Manners et al. [14] reported a DWI and T_2-weighted echoplanar MRI study comprising 10 sCJD patients. At postmortem, the sCJD patients were evaluated for semiquantitative assessment of gliosis and neuronal loss, spongiform changes, and abnormal PrP protein deposition in 4 cortical regions (occipital, parietal, temporal cortex and cingulate gyrus), the thalamus and the striatum, for a total of 60 regions of interest. Results suggested that antemortem reductions in the apparent diffusion coefficient values, typically observed in patients with sCJD, correlate with spongiform changes observed at autopsy. This was clearly established in the striatum and thalamus of the present sCJD patients, in which the extent of spongiform change did not significantly correlate with gliosis or neuronal loss. The study by Manners et al. [14] was based on extremely detailed examination and referred to one of our studies. However, the pathological characteristics of CJD180 differed in our study compared with sCJD. The pathological characteristics of CJD180 included greater spongiform changes, as well as less deposition of abnormal prion protein and astrocytic gliosis compared with sCJD.

The greatest difference between the study by Manners et al. [14] and ours is the concept. In our study, DWI signals from CJD patients were high or low during the clinical course of disease, and these signal changes were detectable.

Due to ethical considerations, brain biopsies were not performed in all cases in the present study. Therefore, the present hypothesis was addressed by supplementary biochemical analysis of CSF and neuroimaging.

Several reports have described the MRS results in CJD patients [15, 16]. NAA is produced exclusively in neuronal mitochondria and reduced levels of NAA are considered to reflect neuronal loss or dysfunction. In turn, Cho levels reflect membrane synthesis and graduation. MI is thought to be located only in glial cells and is, therefore, considered to be a glial marker. A previous report described that reduced levels of NAA correlate with histological neuronal loss and astrocytic gliosis in CJD patients. Some studies have reported reduced NAA levels as a feature of sCJD followed by spongiform changes accom-